Trapping of submicron and micron-sized particles using innovative induced-charge electrokinetic flow

C. Zhao & C. Yang
School of Mechanical and Aerospace Engineering,
Nanyang Technological University, Singapore

Abstract

Microfluidic manipulation of particulate matters has found its applications in cell handling, virus detection, biomolecule concentration and colloidal particle assembly etc. In the literature, optical tweezing, electrophoresis, and dielectrophoresis are well-established techniques for particle manipulations, but these techniques have their respective limitations such as low throughput and high costs for optical tweezing, charged particles required for electrophoresis, complex electrode design for dielectrophoresis. Induced charge electrokinetic (ICEK) flows belong to a new class of flows. One of the basic features for ICEK is the generation of vortices over polarisable surfaces. In literature, these kind of nonlinear vortical flows naturally lend themselves to the mixing enhancement in microfluidic devices. Other than the microfluidic mixing, the applications of induced-charge electrokinetics in microfluidics are very rare. Here a novel and high-throughput technique relying on the induced-charge electrokinetics is proposed and demonstrated for simultaneous trapping and concentration of submicron- to micron-sized particles. The fabricated microfluidic device is simply composed of a straight channel and a gold patch on the bottom wall of channel. Under DC-biased AC electric driving voltages, the trapping of particles over the edge of the conducting gold patch are achieved. Moreover, systematic studies are conducted to investigate the effects AC frequency, AC amplitude, DC offset and particle size on the performance of trapping and concentration by ICEK. In addition, a numerical model is developed to explain the underlying mechanisms of particle trapping via ICEK.
Keywords: induced-charge electrokinetic flow, induced charge electrokinetics, microfluidics, colloidal particle trapping and concentration.

WIT Transactions on Engineering Sciences, Vol 82, © 2014 WIT Press
www.witpress.com, ISSN 1743-3533 (on-line)
doi:10.2495/AFM140221

1 Introduction

Microfluidic technologies have been widely demonstrated with the potential of accurate and fast analyses/diagnoses in biological and chemical sciences as well as drug discovery. Microfluidics aims to integrate multiple steps of analyte manipulations in conventional analyses, such as sample concentration, pumping, mixing, chemical reactions, separation as well as detection etc. into a single microchip. However, due to extremely small volumes of analytes of about nanoliter or less usually used in microfluidic analyses, original low concentration of analytes would lead to poor detection which is one of challenges faced by the microfluidics-based analytical systems [1]. To overcome this challenge has necessitated the pre-concentration of dilute samples prior to further manipulations, detection and analysis. Additionally, practical applications frequently demand the concentration of particulate materials, such as the enrichment of tumor cells for cancer detection [2] and the enrichment of colloidal particles [3] for colloid crystal assembly.

The present study reports the use of so-called induced-charge electrokinetic (ICEK) phenomena as a new means for trapping colloidal particles. The mechanism of surface change modulation with ICEK is resulted from the electric polarization which can be actively tuned by external electric field. Hence, the charge modulation mechanism in ICEK phenomena is different from that due to physiochemical properties of the solid–liquid interface in the conventional electrokinetics dealing with insulating surfaces [4]. When an initially uncharged conductor immersed in the electrolyte solution is subject to an external electric field, the conductor is electrically polarised. Simultaneously electric charges are induced and distributed over the surface of the conductor to ensure equipotential. Subsequently, the induced charge on the conductor surface attracts counterions in the electrolyte solution, leading to the formation of an EDL near the conducting surface. Generally, changes in the strength of external electric field would modify electric polarization of the conductor, and hence the surface charge. In literature, the ICEK phenomena were reported in the colloid science community with focus on flow field around polarised colloidal particles in the presence of external electric field [5]. Recently, Bazant and co-worker [6, 7] revisited ICEK phenomena with emphasis on microfluidic applications. They conceptualised that ICEK phenomena introduce a variety of useful effects that can be beneficial to microfluidics. So far ICEK phenomena have been demonstrated for several microfluidic applications, such as pumping [8], demixing [9], mixing [10], focusing [11] and particle manipulations [12].

Here we present a microfluidic method and device using ICEK phenomena for trapping and concentration of colloidal particles. The device has been tested to examine parametric effects. Additionally, a numerical model is developed to clarify the experimental phenomena to reveal the underlying physical mechanisms of ICEK trapping of particles.

2 Experimental section

2.1 Microfluidic device design and fabrication

The microfluidic device consists of two parts shown in fig. 1(a): a PDMS microchannel and a glass slide deposited with a conducting gold patch. The dimensions of the PDMS channel and the gold patch are illustrated in fig. 1(b). The depth of microchannel is 40 μm and two PDMS cylindrical reservoirs with radii of 6 mm are punched using a puncher (Uni-Core, Harris). To minimize possible dissolution of conducting patch due to electrochemical reactions, noble metal gold is chosen for the conducting patch. In our experiments, the gold conducting patch floats in an external electric field and, then electric charge is induced on the conducting patch and associated induced-charge electrokinetic phenomena occur over the conducting patch to trap the particles.

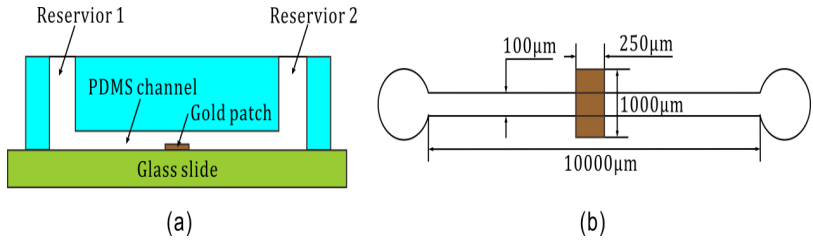

Figure 1: Schematic of the microfluidic device for particle trapping. (a) Cross-sectional view of the microfluidic channel. (b) Top view of the device and dimensions of the channel and the gold patch.

The standard photolithographic technique was adopted to fabricate the PDMS channel. The fabrication of the conducting patch was achieved using the standard lift-off process. Then the PDMS channel and the glass slide with the patterned gold conducting patch were placed into a plasma cleaner (Harrick Plasma Cleaner PDC-32G) for the oxygen plasma treatment of 30s. After that, the PDMS channel and the glass slide were brought into contact to form an irreversible bonding. In addition, the conducting patch was precisely aligned to the center of the microchannel under a microscope during the bonding process.

2.2 Preparation of particle samples

In experiments, green fluorescent polymer microspheres (Thermoscientic, USA) of five different sizes (0.3μm, 0.5μm, 0.7μm, 1μm and 1.9μm) were used. The original particle solutions were all diluted with the 10^{-4}M KCl solution for 250 times, and the final particle concentration in the solution is 0.04 ‰ wt for all cases. Before loading the tested particle solution into the microchannel, the particle suspensions were well mixed and thoroughly stirred in an ultrasonic cleaner (Elmasonic E30H, Elma®) to ensure an excellent homogeneity.

2.3 Experimental system, detection and image analysis

Experiments were carried out with a fluorescence microscope (Axiostar Plus 1169-149, Carl Zeiss) equipped with a long-working-distance 20×objective, a mercury arc lamp (Leistungselektronik mbq 52 AC-Z/ HBO 50 AC), and an appropriate filter set (excitation, 546 ± 12 nm, emission, 600 ± 40 nm). All images were acquired by using a CCD camera (SamBa EZ-140c, Sensovation AG) of 8-bit, 696×520 pixels with a frame grabber (Sensovation SamBa EZ-series IEEE 1394a). To obtain a combined AC and DC voltage for trapping the particles, a function generator (AFG3102, Tektronix) was used to generate a DC-biased AC signal which was then amplified to the desired combination of AC and DC voltage by a customized three channel voltage amplifier (OPT3-AC800-DC1.5K, Optrobio, Singapore). At the same time, the signal of DC-biased AC voltage after amplification was monitored by an oscilloscope.

The tested chip is placed under the microscope with two platinum wires (0.5 mm in diameter, Sigma-Aldrich) placed in each reservoir to apply the amplified voltages. The left platinum electrode was supplied with a DC-biased AC voltage ($V_0+V_1\cos(2\pi ft)$, where f is the AC frequency, V_1 is the AC amplitude and V_0 is the DC voltage) and the right electrode was grounded. Before experiment, two reservoirs were carefully balanced to eliminate the pressure-driven flows.
During experiment, the background was blackened and the green fluorescence particles were illuminated by the blue light from the mercury lamp. The CCD camera was set to the continuous mode to capture the entire process of particle trapping with the time internal between two successive frames about 67 ms. The captured images were recorded in a personal computer for further analyses. The fluorescent intensity was extracted from the images by using an open source image processing software (Image J 1.45) by National Institutes of Health, USA.

2.4 Results and discussion

2.4.1 Trapping of particles of various sizes

Trapping of particles of various sizes is demonstrated in fig. 2. It is obvious that particles get trapped over the right edge of the conducting patch as time elapses. The trapped particles form a line defined by the edge of the conducting patch. The trapping involves two scenarios: at first, the particles are transported from the left to the right by the joint effect of electrophoresis and electroosmotic flow (as denoted by the arrow) due to the DC voltage (note that the AC field does not generate any net flow or particle motion). When the particles reach the right edge of the conducting patch, the induced-charge electrokinetic flow there together with the electrophoresis and dielectrophoresis traps the particles. It is believed that the vortical flow due to induced-charge electrokinetics is the dominant mechanism for the particle trapping [13]. The later theoretical analysis shows that the microvortex forms a stagnant zone where the particles transported from the upstream are accumulated.

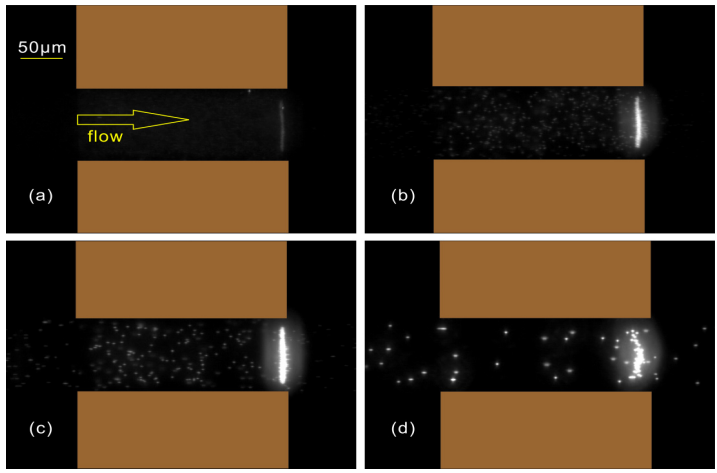

Figure 2: The steady trapping of fluorescent particles over the right edge of the conducting patch after switch on the electric field (V_0=36V, V_1=368V and f=4 kHz) for 30s. (a) 0.3μm, (b) 0.7μm, (c) 1μm, (d) 1.9μm. Two rectangles in each picture define the location of the conducting patch, in between the rectangles there is the microchannel.

The results show that the proposed method can achieve stable trapping of particle from 0.3μm to 1 μm. It is shown that the trapped particles for 0.3 μm, 0.7 μm and 1 μm form straight lines which are defined by the right edge of conducting patch. For 1.9 μm particles, trapped particles are more spread as compared to other three smaller sizes. This could be due to the fact that induced-charge electrokinetic vortices are not strong enough to catch such large particles.

2.4.2 Effects of relevant parameters on the trapping performance

Fig. 3 presents the effects of combined AC and DC field on the trapping performance. The vertical axis in each plot denotes the fluorescent intensity which is an indication of the particle concentration. The higher the fluorescence intensity is, the higher the particle concentration is. As shown in fig. 3(a), the band of trapped particles under a lower AC frequency is more spread. As the AC frequency increases, the band of trapped particles is compressed to the right edge of the conducting patch. It is clear that there exists an optimal frequency at which the band accumulates the most particles. The effect of the AC amplitude on particle trapping is monotonic, as can be seen from fig. 3(b). The band of trapped particles becomes narrower as the AC amplitude decreases. With increasing DC offset, the electroosmotic flow becomes stronger, which pushes the band of trapped particles to the right edge of the conducting patch (see fig. 3(c)). The investigation also predicts an optical DC offset under which the band traps the most particles. This should be understandable, because if the DC offset is mall, electroosmotic flow is not strong enough to transport sufficient particles to

the trapping zone; while if the DC offset is too high, electroosmotic flow is so strong that the trapped particles are washed off from the edge of the conducting patch.

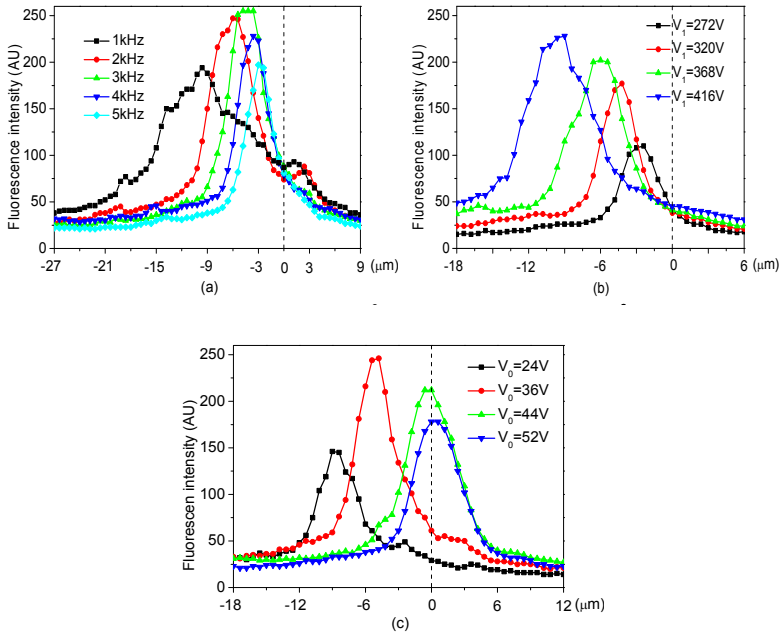

Figure 3: Effects of the combined AC and DC electric field on the steady-state trapping of 500nm fluorescent particles. All fluorescence intensity profiles are along the center line of the 100μm wide microchannel. Vertical dash lines represent the right edge of the conducting patch. (a) Effect of AC frequency on the particle trapping when DC V_0=36V and AC V_1=368V. (b) Effect of AC amplitude on the particle trapping when DC V_0=36V and AC f=4 kHz. (c) Effect of DC offset on the particle trapping when AC V_1=368V and AC f=4 kHz.

3 Numerical modeling of ICEK particle trapping

3.1 Simulation domain and formulation of the problem

Since the channel width (100μm) in the experiment is 2.5 times of the channel depth (40μm), the simulation domain can be effectively represented by a rectangular domain shown in fig. 4 (a two dimensional cross-section along the depth direction of the microchannel). Specifically, the segment CD with length of 2L at the center of the lower boundary denotes the conducting patch, segments BC and DE are the glass walls, and segment AF is the PDMS wall. In the

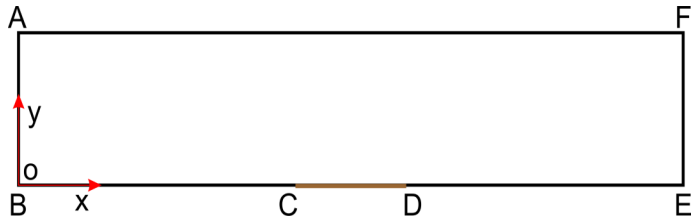

Figure 4: Sketch of the modeling domain. Segment CD represents the gold conducting patch, BC and DE are the lower glass walls and AF is the upper PDMS wall.

simulation, BC and DC are chosen to be at least 10L long to minimize the effects of inlet and outlet boundaries (AB and FE) on the simulation results.

The numerical model of particle trapping consists of three governing equations describing the mass transport of particles, the induced-charge electrokinetic flow field, and the induced zeta potential on the conducting surface. We introduce the following scales for the nondimensionalization of governing equations, $[x, y] = L$ and $[\phi] = k_B T / ze$. Here L is half width of the gold patch, k_B is Boltzmann constant, T is temperature, e is elementary charge, and z is the valence of electrolyte ions. It is assumed that the microchannel wall does not adsorb particles and there is no interaction among particles. The particle concentration can be governed by the mass transport equation in dimensionless form.

$$\frac{\partial c}{\partial t} + Pe\nabla \bullet \left[\left(\mathbf{u} + \mathbf{u}_{ep} + \mathbf{u}_{dep} \right) c \right] = \nabla^2 c \tag{1}$$

in which the scales of time, particle concentration and the Peclet number are respectively defined as $[t] = L^2 / D_p$, $[c] = c_0$ and $Pe = [\mathrm{u}] L / D_p$. Here, the concentration scale c_0 is the initial particle concentration, and D_p is the particle mass diffusivity which can be estimated from the Stokes-Einstein relation, $D_p = k_B T / 6\pi\mu a$, with a being the radius of the particle. Eqn (1) indicates that beside the ICEK flow, other electrokinetic forces (electrophoresis and dielectrophoresis) also contribute to particle transport. The time scale analysis suggested that concentration field dominates the transient characteristics of the whole system [14]. Hence the transient term is only present in the mass transport equation. The electric and flow problems can be treated as pseudo-steady. Due to a combination of AC and DC electric field, the electric problem can be formulated in terms of phasor variables. The dimensionless complex amplitude of electric potential in the bulk fluid satisfies

$$\nabla^2 \phi_f = 0 \tag{2}$$

The boundary condition over the surface of floating conductor is given as [4, 13]

$$\phi_f - \phi_c = \frac{d\phi_f}{dy}\frac{1}{j\omega\tau\sqrt{1+j\omega\tau\left(\lambda_D / L\right)}} \tag{3}$$

Note that $\tau=\lambda_D L/D_i$ represents the characteristic time scale for the double layer changing over the conducting patch, or the so-called "RC time" in the terminology of the equivalent circuit. In the definition of τ, D_i is ionic diffusivity, and λ_D is the Debye length and is defined for a symmetric (z:z) electrolyte as $\lambda_D = \sqrt{\varepsilon_0\varepsilon_f k_B T / \left(2n_\infty e^2 z^2\right)}$, where $\varepsilon_0\varepsilon_f$ is the electric permittivity of the electrolyte solution and n_∞ represents the bulk ion concentration. $\omega=2\pi f$ is the angular frequency of the electric field. It should be noted that for a floating conductor with perfect polarizability, it is polarized instantaneously after the application of external electric field and remains equipotential with ϕ_c in the entire charging process of the electric double layer.

Then the total potential drop across the double layer, or equivalently the zeta potential over the conducting surface, can be evaluated as

$$\zeta = \phi_c - \phi_f \tag{4}$$

Once the double layer around the conductor is charged, the externally applied field exerts a body force on ionic charge in the double layer, driving the ions and then the liquid into motion. For the thin EDL situation considered here, the resultant electrokinetic flow appears to slip just outside the double layer and the slip velocity varies proportionally to the local electric field strength and is given by the Helmholtz–Smoluchowski equation

$$\mathbf{u} = \left\langle \zeta \nabla \phi_f \right\rangle \tag{5}$$

where $\langle\cdots\rangle$ denotes the time averaging. Eqn (5) is the boundary condition over the conducting patch and the channel walls for the time averaged flow field.

Usually, the flows considered in microsystem are usually of creeping type due to very small Reynolds number, and then the equations governing the ICEK flow of an incompressible liquid are the continuity equation and the Stokes equation

$$\nabla \bullet \mathbf{u} = 0 \tag{6}$$

$$-\nabla p + \nabla^2 \mathbf{u} = 0 \tag{7}$$

together with slip velocity on the solid surface as given by eqn (5) [13].

Velocity and pressure is made dimensionless by following natural scales

$$[u] = \varepsilon_0\varepsilon_f[\phi]^2 / \mu L \qquad [p] = \varepsilon_0\varepsilon_f[\phi]^2 / L^2 \tag{8}$$

where μ is the dynamic viscosity of the electrolyte solution.

Electrophoresis resulted from the interaction of the electric field with the charged particles. For a negatively charged particle in a bulk fluid, the electrophoretic force drags the particle from the cathode side of the electric field to the anode side of the electric field. For particles with thin EDLs, the time averaged electrophoretic velocity is expressed as

$$\mathbf{u}_{ep} = -\zeta_p \left\langle \nabla \phi_f \right\rangle \tag{9}$$

where ζ_p is the dimensionless zeta potential for particles.

The presence of the floating conducting patch can perturb local electric field, and hence creates a nonuniform electric field around the conducting patch. Dielectrophoretic force is generated due to the interaction of such non-uniform electric field with the dipole moment induced by the same field inside a polarizable particle. The resulting dielectrophoretic force can transport the particle from high (low) electric field strength to low (high) electric field strength, depending on electric properties of particles and surrounding media. The time averaged dielectrophoretic velocity of particle $\mathbf{u}_{dep}$ is expressed as

$$\begin{aligned}\mathbf{u}_{dep} = \frac{1}{3}\left(\frac{a}{L}\right)^2 \mathrm{Re}\left[\underline{K}(\omega)\big|_{\omega\to 0}\right]\nabla\left(\left\langle\nabla\phi_f\right\rangle\bullet\left\langle\nabla\phi_f\right\rangle\right) \\ + \frac{1}{3}\left(\frac{a}{L}\right)^2 \mathrm{Re}\left[\underline{K}(\omega)\right]\nabla\left[\left\langle\left(\nabla\phi_f - \left\langle\nabla\phi_f\right\rangle\right)\bullet\left(\nabla\phi_f - \left\langle\nabla\phi_f\right\rangle\right)\right\rangle\right]\end{aligned} \tag{10}$$

where the Clausius-Mossotti (CM) factor is defined as $\underline{K}(\omega) = \left(\underline{\varepsilon}_p - \underline{\varepsilon}_f\right) / \left(\underline{\varepsilon}_p + 2\underline{\varepsilon}_f\right)$. The complex dielectric permittivities of the particle and electrolyte solution are $\underline{\varepsilon}_p = \varepsilon_0\varepsilon_p - j\sigma_p/\omega$ and $\underline{\varepsilon}_f = \varepsilon_0\varepsilon_f - j\sigma_f/\omega$, respectively, with $j = \sqrt{-1}$. The particle has an electric permittivity of $\varepsilon_0\varepsilon_p$ and a conductivity of σ_p. The conductivity of particle consists of the bulk conductivity and the surface conductivity ($2\sigma_s/a$). For latex particles, the bulk conductivity is usually taken to be zero and the surface conductance σ_s ranges from 0.2 to 2.1nS [13]. The first term in eqn (10) denotes the DC dielectrophoretic velocity of particle due to the DC component of the electric field and the second term is the AC dielectrophoretic velocity of particle.

3.2 Numerical method and boundary conditions

Table 1 lists the boundary conditions specified for three governing equations. The finite-element software (Comsol Multiphysics 3.4) is used to simulate the particle trapping due to induced-charge electrokinetics. The whole computational domain was meshed with triangular elements, and the mesh near the conducting patch CD was the finest to capture large gradients in this area. The grid independence was also tested. The electric problem and the flow problem were first solved sequentially using the stationary UMFPACK solver with a relative tolerance of 10^{-6}. The particle concentration was then solved using the converged results of the electric and velocity fields by a time-dependent BDF solver.

3.3 Numerical simulation results

Fig. 5 presents the numerical predictions of three different hypothetical cases for trapping of 1 μm particles at the steady state. Fig. 5(a) presents the first hypothetical case without the floating conducting patch. It is expected that the

Table 1: Summary of the boundary conditions for governing equations of electric problem, flow problem and mass transport problem.

Boundary segment	Electric problem	Flow problem	Mass transport
AB	Specified voltage	Zero pressure	Specified
BC	Insulation	Slip velocity	Impermeable
CD	Charging of EDL	Slip velocity	Impermeable
DE	Insulation	Slip velocity	Impermeable
FE	Grounded	Zero pressure	Convective flux
AF	Insulation	Slip velocity	Impermeable

typical flow field under this case is an electroosmotic plug flow in the microchannel. The particle transport in this case is due to the effect of both electroosmotic plug flow and particle electrophoresis. It is seen that the particle concentration is uniform in the entire channel domain, with its initial normalized value of unity. Fig. 5(b) depicts the second hypothetical case with the induced-charge electrokinetic flow but without consideration of the particle dielectrophoresis. In this situation, two vortices over two edges of the conducting patch are generated because of induced-charge effects. There is still no trapping of particles as shown in fig. 5(b). Only when both induced-charge electrokinetic flow and dielectrophoresis are effective (fig. 5(c)), the particles can be trapped and concentrated in a region defined by the ICEK microvortex over the right edge of conducting patch. The results from the three hypothetical cases suggest that ICEK flow and particle dielectrophoresis are both crucial for successful trapping of particles. Based on this picture, the trapping mechanism can be understood as follows: the dielectrophoresis only takes effect very near the edges of conducting path and try to trap the particles on the edge of the conducting path (Note that 1 μm particle experience positive dielectrophoretic force which pushes particles to the edges of conducting patch). Subsequently, induced-charge electrokinetic flow entrains these trapped particles into the vortex, leading to the final trapping of particles. Interestingly, the trapping of particles only occurs inside the right vortex, which can be attributed to the DC field driven electroosmotic flow from the insulating channel which breaks the symmetric configuration of two vortices generated by pure ICEK. In the modeling, it is found that the trapping location shifts to the left vortex if the polarity of the DC field is reversed, which is also consistent with our experimental observations.

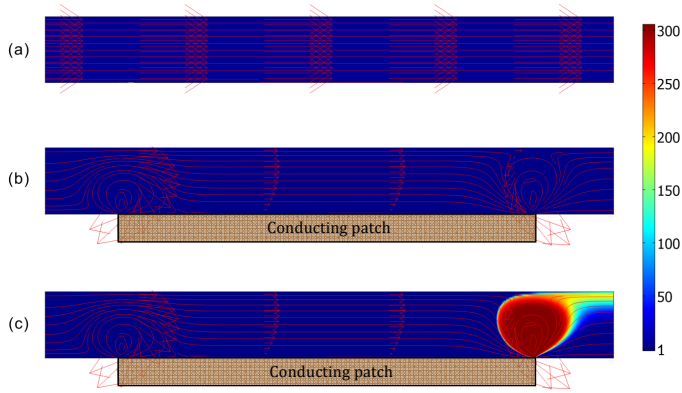

Figure 5: Numerical predictions for the steady-state trapping of 1μm particles under a combined AC and DC electric field (V_0=36 V, V_1=368 V and f=4 kHz). (a) Without the conducting patch (i.e., without ICEK flow and dielectrophoresis), (b) Without dielectrophoresis and with ICEK flow, (c) With both ICEK flow and dielectrophoresis. The arrows and lines give details of flow field and the contour plots give the normalized particle concentration field.

In summary, the presented model can only give qualitative prediction of the particle trapping. Those discrepancies between the precautions and experiments can be possibly explained from two aspects: first, for the theoretical prediction of induced-charge electrokinetic flow, the velocity from the experiment is always lower than that from the theory in most existing literature, sometimes even by orders of magnitudes [7]. The reason for this may be manifold, such as ion crowding in the EDL, surface contamination and increased viscosity of the solution near the solid surface. Second, in the modeling of particle transport, the mass flux of particles due to other colloidal forces, such as EDL forces among particles, van der Waals force among particles were neglected. These forces are important when the interparticle distance becomes small.

4 Concluding remarks

We proposed a novel method for particle trapping via the induced-charge electrokinetics. It is demonstrated that the proposed method is capable of trapping particles with size ranging from 0.3 μm to 1.9 μm. In addition, a multiphysical model is developed to illustrate the trapping mechanism. The particle transport due to the induced flow, electrophoresis and dielectrophoresis is solved to obtain the particle concentration field. It is shown that the induced-charge electrokinetic flow circulation and dielectrophoresis over the edge of the conducting patch are indispensable to the successful trapping of particles, and there would be no trapping if either of them disappears. Only a qualitative agreement between the theoretical predictions and experimental results is

achieved because of assumptions and limitations in the model, and more advanced models will be required to get good agreement.

References

[1] Crompton, T.R. Preconcentration Techniques for Natural and Treated Waters: High Sensitivity Determination of Organic and Organometallic Compounds, Cations and Anions. London, Taylor & Francis, 2002.
[2] Alix-Panabieres, C. & Pantel, K., Technologies for detection of circulating tumor cells: facts and vision. Lab Chip **14**, pp. 57-62, 2014.
[3] Cong, H., Yu, B., Tang, J., Li, Z. & Liu, X., Current status and future developments in preparation and application of colloidal crystals. Chem. Soc. Rev. **42**, pp. 7774-7800, 2013.
[4] Zhao C., & Yang C., Advances in electrokinetics and their applications in micro/nano fluidics Microfluid. Nanofluid. **13**, pp. 179-203, 2012.
[5] Gamayunov N.I., Murtsovkin V.A. & Dukhin A.S., Pair interaction of particles in electric field. 1. Features of hydrodynamic interaction of polarized particles. Colloid J. USSR **48**, pp. 197-203, 1986.
[6] Bazant M.Z. & Squires T.M., Induced-Charge Electrokinetic Phenomena: Theory and Microfluidic Applications Phys. Rev. Lett. **92**, 066101, 2004.
[7] Bazant M.Z. & Squires T.M, Induced-charge electrokinetic phenomena Curr. Opin. Colloid Interface Sci. **15**, pp. 203-13, 2010.
[8] Gregersen M.M., Okkels F., Bazant M.Z. & Bruus H., Topology and shape optimization of induced-charge electro-osmotic micropumps New J. Phys. **11**, 075019, 2009.
[9] Leinweber F.C., Eijkel J.C.T., Bomer J.G. & van Den Berg A., Continuous flow microfluidic demixing of electrolytes by induced charge electrokinetics in structured electrode arrays Anal. Chem. **78**, pp. 1425-34, 2006.
[10] Wu Z.. & Li D. Mixing and flow regulating by induced-charge electrokinetic flow in a microchannel with a pair of conducting triangle hurdles Microfluid. Nanofluid. **5**, pp. 65-76, 2008.
[11] Dhopeshwarkar R., Hlushkou D., Nguyen M., Tallarek U. & Crooks R.M., Electrokinetics in microfluidic channels containing a floating electrode J. Am. Chem. Soc. **130**, pp. 10480-1, 2008.
[12] Gangwal S., Cayre O.J., Bazant M.Z. & Velev O.D., Induced-charge electrophoresis of metallodielectric particles Phys. Rev. Lett. **100,** 058302, 2008.
[13] Zhao C., & Yang C., Analysis of induced-charge electro-osmotic flow in a microchannel embedded with polarizable dielectric blocks Phys. Rev. E **80**, 046312, 2009.
[14] Ge Z.W., Yang C., & Tang G.Y., Concentration enhancement of sample solutes in a sudden expansion microchannel structure with Joule heating. Int J Heat Mass Transfer, **53**, pp. 2722-2731, 2010.